DESIGN OF A "LARGE" UNMANNED AERIAL VEHICLE FRAME FOR METAL ADDITIVE MANUFACTURING ON THE AEROSWIFT MACHINE

J.V Prinsloo[1*], N.J. Minnaar[2] and M.Vermeulen[1]

ABSTRACT

In order to demonstrate the capability of manufacturing a large-scale aerospace part, it was envisioned to design an Unmanned Aerial Vehicle (UAV) frame which would fit into the Aeroswift build volume. The Aeroswift machine is a metal powder bed fusion system with a large build volume. In this paper, the complete design process of a UAV frame will be outlined and the optimization methodology followed to reach an optimized design solution will be covered in detail.

[1] ADC Aeroswift, South Africa (Corresponding author) j.prinsloo@aeroswift.com

[2] Altair Engineering, South Africa nminnaar@altair.co.za

INTRODUCTION

An Unmanned Aerial Vehicle (UAV) is an aircraft without a human pilot aboard. The flight is controlled either autonomously by onboard computers or by the remote control of a pilot on the ground or in another vehicle [1].

The Aeroswift machine was designed and developed by Aerosud Innovation Centre in partnership with the Council for Scientific and Industrial Research (CSIR) and funded by the Department of Science and Technology (DST). The Aeroswift project was started in 2008, with the goal of manufacturing aerospace parts in Ti6Al4V for aerospace and other industries. The Aeroswift system has a build volume of 2000mm x 600mm x 600mm and is thus capable of manufacturing large-scale parts. The design of the UAV frame will serve as an aerospace technology demonstrator for the powder bed fusion process on a large platform system such as the Aeroswift machine. The project aims to demonstrate that topology optimization can be used to optimize the design of a large UAV frame and that the Aeroswift system is capable of manufacturing a complex and large scale part.

The key areas of the design process have been defined as UAV craft requirement specification, electronic component and drivetrain selection, mechanical design employing topology optimization techniques, aesthetic improvements and manufacturability improvements.

1. FRAME DESIGN

1.1 UAV craft and frame requirements

The project started with specifying the requirements of the functional UAV craft and frame as the following:

- The frame should fit into a 320 x 600 x 560 mm^3 build volume
- The UAV should have symmetrical motor placement.
- Flight times of at least 15 minutes should be achieved.
- Components should be included for autonomous flight capability, stabilized video recording and First Person View (FPV) capability.
- The fully constructed UAV should have a thrust to weight ratio of at least 2.5:1.
- The design must consider camera viewing angles in order to ensure unobstructed video footage.
- The final frame design should be producible with the powder bed fusion AM process in Ti6Al4V.
- Frame stiffness should be maximized.
- Aesthetics should be considered during the design process.

1.2 Component selection

A UAV craft requires a core set of components, i.e. Motors, propellers, electronic speed controllers, a flight controller and a battery in order to be functional [2]. In addition to the core components, additional components such as cameras, camera gimbal and communication are required to satisfy the requirements as described in the previous section.

1.2.1 Motors

The motors are the source of power, to spin the propellers, for the UAV craft. Brushless direct current (DC) motors are most commonly used for this type of application. A brushless motor consists of a core stator and bell with permanent magnets on the inside of the bell. The stator, which is essentially an electric magnet, generates a magnetic field in such a way that the permanent magnets are moved in a sequence to sustain the rotational speed

of the motor. Brushless motors are favoured over Brushed DC motors because of their increased torque, reduced noise, reliability, and higher efficiency [2]. Usually, a UAV craft requires multiple motors to supply the total power required for sustained flight.

1.2.2 Propellers

The propellers, which are attached to the motor bell, convert the rotational spin of the motor bell to downward force or thrust. A propeller can be characterized in terms of its diameter and the pitch of the blades. Even though there is a very wide range of propeller sizes and pitches available, the size of the UAV frame and the specifications of the motors limit the range of propellers that can be used on a specific UAV craft. The manufacturer of the motors will also specify the range propeller sizes and pitches to be used to operate a motor safely, achieve maximum performance and efficiency.

1.2.3 Electronic speed controllers

Due to the high current and voltage requirements of the motors, the electrical power to the motors can't be supplied by the flight controller. Electronic speed controllers are required to handle this task. The electronic speed

controllers control the rotational speed of the motors. These components typically use pulse width modulated signals to vary the voltage and current required by the motor to in turn control the speed. The control signal is connected to the flight controller in order to manage the trust generated by each motor.

1.2.4 Battery

The battery is the electrical power supply for the entire electrical system and drivetrain. Depending on the power rating of the battery a UAV craft can be operated with a single battery pack or a battery bank, depending on the lifting capacity of the craft and the available space. Lithium-polymer (Li-Po) batteries are the most popular to use in this type of application. Li-Po batteries are light-weight, rechargeable, has a high power density and the ability to provide the high sustained current output required for the motors. A Li-Po battery is characterized by its capacity and the cell count.

1.2.5 Flight controller

The flight controller is the control system of the UAV craft. The basic hardware components on a flight control board are a microcontroller, gyroscope sensor and accelerometer. A number of other sensors can be added to a flight controller to provide feedback about the operating environment, collision avoidance and to aid in autonomous control functions. The control software or firmware that executes on the flight control board constantly reads the sensor data, performs data filtering, processes data in control algorithms and outputs control signals to the motors. The control algorithms constantly make slight changes to the rotational speed of the motors (at high sample rates) to balance out the thrust vectors, perform manoeuvres and ultimately sustain stable flight.

1.2.6 Camera and stabilization gimbal

The usage of cameras on a UAV craft can have two roles, one being to record footage from the UAV and the other to provide the pilot with a first-person video (FPV) view from the UAV craft. There are cameras available on the market that is able to function as a recording camera and as an FPV camera in some applications where 2K or 4K video recording is not a requirement.

Due to the vibrations generated by the spinning motors and propellers, unwanted or blurred lines will be seen in the camera footage. To counteract the vibrations, a gyroscopically controlled gimbal can be used to provide a stable platform for the recording camera to ensure vibration free video recordings.

1.3Drivetrain selection

The most important aspects to address early in the design were frame weight, the size and number of motors to use and battery size. The flight controller, cameras, camera gimbal/mounts and other control and communication electronics which would satisfy the functional requirements of the UAV craft also had to be specified. All non-drivetrain electronic components required in the craft were selected in order to calculate the all up weight of the craft, to determine mount point locations and subsequent design space limitations.

Hexacopter (six motors) and quadcopter (four motors) configurations were considered. In order to satisfy the thrust to weight and flight time requirements with the specific frame size, it was decided to pursue a quadcopter configuration for this design.

1.3.1 eCalc benchmark tool

To aid in the design and selection process, a comprehensive and specialized calculation tool and component database, namely eCalc [3] was used. The eCalc tool benchmarks the frame, motor, propeller and battery configuration and estimates a number of performance values. The eCalc tool can be used to compare different drivetrain setups and performance metrics are based on the performance data of the actual components. The eCalc tool is widely known and used for benchmarking non-commercial or custom developed aircraft to estimate performance statistics of the frame and drive train components [1],[4],[5].

With the number of motors and the maximum allowable frame size known an iterative process could be followed to determine the drive train components required to satisfy the flight time and thrust requirements. Due to the vast number of available components in the eCalc database, the focus was placed on reputable component vendors as well as components that are readily available. It was not required to find the optimal drive train setup but only satisfy the flight time and thrust requirements.

1.3.2 eCalc estimation results

The results obtained by the eCalc tool can be shown in Figure 1.

Figure 1: UAV craft eCalc results.

As can be seen from Figure 1, the frame weight and size has been entered as 650 g and 750 mm respectively. The eCalc software only needs the size of the frame to determine if the chosen propeller size will fit the frame. A frame size was of 720 mm (measured between diagonal motors) was chosen in order to fit into the 320 x 600 x 560 mm^3 build volume of the Aeroswift machine.

The following components were chosen for the drivetrain:

- Tiger motor MN3110 – 780 Kv motors
- 10000 MAh four cell Li-Po battery
- Dual blade carbon fibre propellers with a diameter of 304.8 mm and a pitch of 101.6 mm.

With this configuration, it was found that a thrust to weight ratio of 2.6 and a flight time of at least 16 minutes can be achieved. This information, together with the component mount positions, were required inputs into the optimization phase of the design.

2. SIMULATION INPUTS

The virtual prototyping that is used to design and evaluate the UAV frame requires various simulation inputs. This section is dedicated to describing those simulation inputs and will commence with a description of the parameters related to the physics of the UAV frame. The parameters relating to the computational solution of the physics are discussed thereafter.

2.1 Physical Parameters

It is necessary to accurately capture the physics of the UAV frame and this is facilitated by defining the following parameters:

- The parameters which characterize the behaviour of the Ti6Al4V titanium alloy to be used for manufacturing. The elastic modulus, poisons ratio and material density are specified as follows: E = 116.5 GPa, Nu = 0.31, Density = 4429 kg/m^3, Yield Stress = 827.3 MPa. It is also noted that the benchmark design, which will be discussed later, was simulated using Nylon. The corresponding material properties are: E = 2.91 GPa, Nu = 0.41, Density = 1230 kg/m^3, Yield Stress = 75 MPa.
- A definition of the loading that will be impressed on the UAV frame. The identified loads represent worst-case scenarios for the constituent loadings that will, when combined
in various combinations, make up any load-case expected to be impressed on the in-flight UAV.

It is noted that in Finite Element Analysis (FEA), in order to analyze structural responses, it is necessary to constrain rigid body motions in the product being analyzed. In reality, however, the UAV experiences an imbalance of forces and torque and this is the mechanism through which motion is achieved. Therefore, it was necessary to perform an equivalent static load (ESL) analysis whereby the analysis reference frame was considered as being fixed to the UAV's centre of gravity (COG) and fictitious inertial loadings were used to balance out the force and torque imbalances that usually result in UAV motion. In this way, the same structural responses that would be exhibited by the in-flight UAV, are simulated for a particular epoch. This is also referred to as an inertia relief analysis.

There are three equivalent static load-cases to represent the most extreme roll, pitch and yaw motions. These are the names given to rotational motions of the UAV around the three body-fixed orthogonal axes aligned with the frame. These motions, along with an illustration of the constituent loads that cause them are shown in Figure 2. A forth load-case to represent the most extreme vertical accent possible was also defined and is also shown in Figure 2. Lastly, negative variants of the roll, pitch and yaw motions were also analyzed.

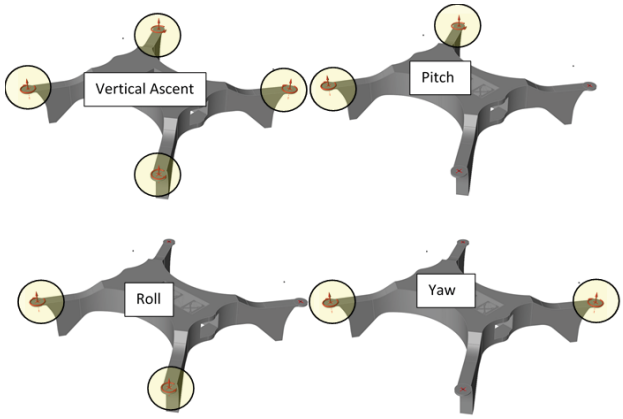

Figure 2: The load-cases for distinct UAV motions.

It was also necessary to define an additional fictitious load to represent a landing scenario. The primary reason for this was to ensure topology generation in the volumes which encompass the landing gear of the UAV. To ensure appropriate topology generation in these regions a connected mass at the extremities of the landing gear was defined (as shown in Figure 3) which needed to be virtually supported through all the other load cases. This alleviates the difficulty of defining a landing load-case since there are many factors to consider for such a loading scenario (eg. angle of attack, descent speed etc.).

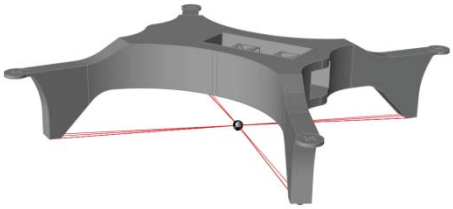

Figure 3: A concentrated mass connected to the landing gear to ensure topology generation.

In Section 4, the reader will encounter curves that depend on numerated load-cases that have been described in this section. Therefore, each load-case is numerated below in order to provide context for those descriptions.

1. Vertical Ascent
2. Pitch
3. Roll
4. Yaw
5. Negative Pitch
6. Negative Yaw
7. Negative Roll

2.2 Computational Parameters

There are factors relating to the computation of results for the simulation that affect the accuracy of the simulations, even if it is assumed that the physics of the UAV frame has been accurately represented. In addition, these computation factors can also affect the length of time required for results to be generated. The computational factors considered are as follows:

- Element Size: During the course of a finite element analysis, a geometric structure is discretized using a finite number of elements (see Figure 4 for an illustration). Each element
- is made up of nodes which in turn represent the number of calculation points for which a solution will be generated by the FE solver. The element sizes were varied in each analysis. Initial runs utilized elements in the range of 12mm while final analyses utilized elements in the range of 1.5mm since numerical accuracy was sought in the concluding phases of the design process.

- Element Order: Any single element may be configured by placing nodes at the vertices of the element only, or by placing nodes at the element vertices and the mid-span of the element edges. These are referred to as first order and second order element, respectively, due to the resulting order of the polynomial equations that represent the field quantities across those elements. Equal size second order elements produce a numerically more accurate solution at the cost of computation time. This project has utilized first order elements throughout.
- Number of assigned CPU cores: The FE solver technology that forms the kernel of Altair Inspire (Optistruct) facilitates parallelization of the FE analysis submitted to it. This capability was utilized during this project as four physical cores were used to run all analysis, resulting in shorter wall-times during analyses/optimizations.
- Topology thickness range: The solution space is constrained by the topological thicknesses that are being considered in the solution. By constraining the solution space with a topological thickness specification, computational times can be reduced substantially. It should be noted that there are rules governing the allowable constraints of topological thicknesses based on the size of the elements employed. The topological thickness constraints varied from 9 mm in the first optimization to 4 mm in the last optimization of the design process.

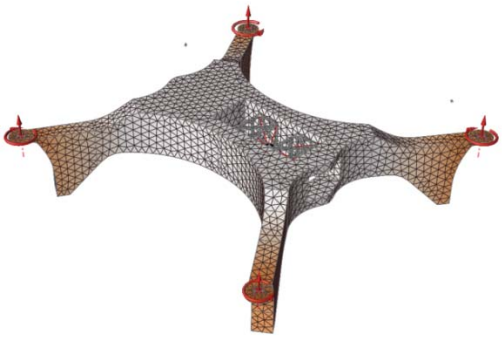

Figure 4: An illustration of the discretization of the UAV frame.

3. TOPOLOGY OPTIMIZATION TECHNOLOGY

Topology optimization (TO) is a mathematical theory which enables the synthesis of structurally optimal products. The basic concepts of the technology will be described below, followed by a description of the components that should make up a TO solution. Lastly, a description of how the technology has been adapted for the Additive Manufacturing (AM) domain specifically will be given.

The layout of material within a volume directly affects the manufacturability, cost, and functional performance of that volume. Designing the material layout for a given volume is therefore complex, and hence best approached in a structured manner. Topology optimization technology is a platform off of which to approach a particular design in such a structured manner. The technology employs an algorithmic approach in which a design concept for material layout within a volume is iteratively modified and gauged for performance in order to inform the modification necessary in the following iteration. The process is repeated until the performance of the design volume has converged within the constraints placed on it [6].

Multiple components should be incorporated into a TO solution. Firstly, the basis of a product designed with TO is a concept design volume which has been created in a Computer Aided Design (CAD) package. The TO solution should, therefore, have open interfaces through which to import these CAD concepts which have been created in other software or it should have native CAD-like capabilities for the generation of a basic concept. Secondly, a TO solution should incorporate FEA capabilities. FEA has traditionally been used for the simulation of the structural behaviour of a designed product. FEA thus provides the mechanism through which to evaluate the performance of each iteration. Lastly, a TO solution should incorporate the appropriate tools for translating the final design concept from the FEA domain into the CAD domain (this is necessary so that the design may be exported from the TO solution and imported into other software in the design/manufacture toolchain). All these components of a TO solution could be found in the Altair Inspire 2018 package which was used during this project for the design of the UAV frame.

Although TO offers designers a tool to synthesize structurally optimal products, the technology does also present its own challenge. The most structurally efficient design is not necessarily the most manufacturable design [7]. To address this challenge, the TO technology can be adapted to account for constraints of the manufacturing process [8]. As an example, and relevant to the additive manufacturing space, a restriction can be added regarding the angle to which consecutive boundary layers of a part are built [9], [10]. This would, in turn, remove the need to create support structures during the build preparation phase.

The angle constraint was only applied during the reduced optimization that is illustrated in Figure 4(g) and not in the other optimizations that were performed. The assumption which drove this decision was that the boundaries created by the reduced optimization (in which subsequent optimizations would search for a final solution) would have been limited to the printable angle ranges, and hence, any topology that would be created within those boundaries would require only minor support within the boundaries themselves. It was found that there still remained the need to support areas in the design but with slight changes in the model, the number of required supports could be reduced greatly.

3.1 Design methodology

Due to specific structural and weight requirements, it was decided to use topology optimization as a tool to optimize the frame design. The design methodology followed is described in the seven steps listed below, whereas the topology optimization technologies themselves are described in Section 3. Where applicable, the outputs of the steps are shown in Figure 5.

1. Baseline concept design was generated, using primitive volumes (rectangles, cylinders, etc.) with as little detail as possible, but including position and mounting info of all components. See Figure 5(a).
2. The primitive/baseline concept was imported into topology optimization software (Altair Inspire in this case) and a baseline finite element method (FEM) analysis was performed to check that loading conditions are correct.
3. A baseline optimization was run to ensure that the generated topology facilitates connections between all the components in the assembly and also that connections of the assembly to important functional interfaces are retained. The result of this step is shown in Figure 5(b).
4. A check was performed to verify if the baseline optimization retained material at the boundaries of the primitive real-estate. This was indeed observed, thus indicating that the design domain needed to be increased in order to capture the load paths in the material more optimally. This is illustrated in Figure 5(c).
5. Topology branch sizes were increased to reduce the computational complexity and the process was repeated to produce the thickest boundaries which encompass the load paths in the material (Figure 5(d)).
6. The design space was reduced and a full-scale optimization was completed where small branch thicknesses were considered. To form a new design space, geometry was created to capture the topology of the baseline optimization from the previous step (Figure 5(e)). Ad-hoc modifications to improve AM manufacturability and aesthetics was done at this step and is shown in Figure 5(f).
7. The final design optimization was completed and the resultant geometry was subsequently recreated with thin thinner, optimized branches (See Figure 5(g)).

3.2 Topology Optimization Results

The methodical process followed in the previous section clearly shows the transformation from a very basic design to a topology optimized design. It was even possible to adapt the aesthetics of the design to take the shape of a butterfly and make it suitable for production in metal AM. (build direction as shown Figure 5(g)). The estimated weight of the optimized design is ~647g. The eCalc estimation used a frame weight of 650g as input and thus the calculated performance values should be accurate with the tolerance specified by the eCalc tool.

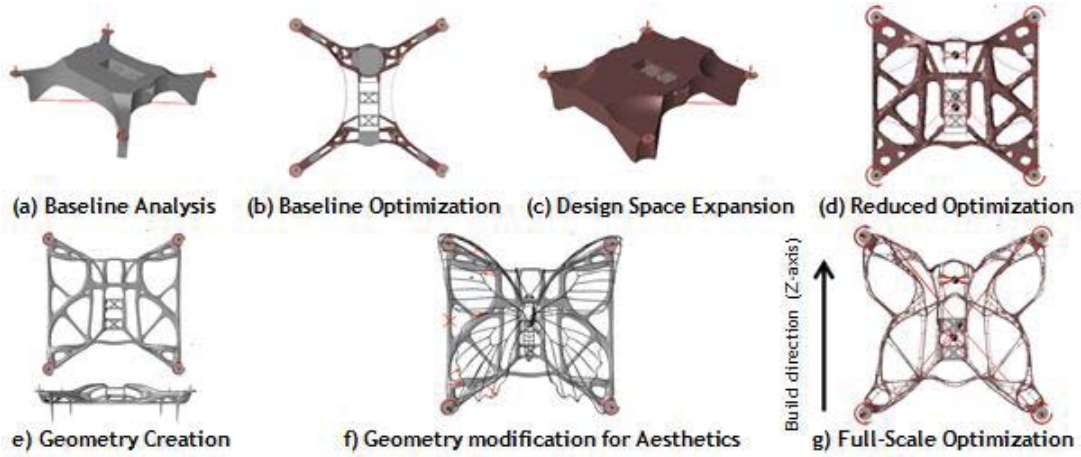

Figure 5: UAV frame design optimization Process.

4. FRAME EVALUATION

4.1 Strategy and Evaluation Metrics

The UAV frame evaluation focus was to determine if the final frame design adheres to the mechanical specifications described in Section **Error! Reference source not found.**. Various metrics can be associated with the UAV frame and it is p ossible to track these metrics through a number of design iterations. Then by comparing these metrics for subsequent iterations with the benchmark (initial concept), it is possible to evaluate whether the design has matured towards an optimal concept or not. The next few paragraphs describe the metrics that were used.

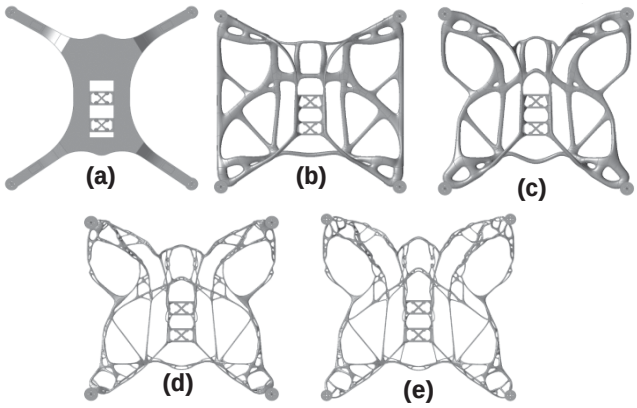

Figure 6: Selected design iterations that are used for evaluation. (a) Benchmark, (b)-(e) Iteration 1 to 4 respectively.

One obvious and valuable metric for evaluating the frame design is its total mass since this metric directly addresses the specification regarding the thrust-to-weight ratio of the UAV. According to the eCalc tool results, the total UAV weight should not exceed 650g. The total mass of the frame must thus be lowered from the baseline concept which has a mass slightly exceeding 1.3kg.

Each frame design iteration has a set of calculable single-values which correspond to the individual load cases and are termed compliances. These compliances describe the strain energy absorption of the frame under the associated load case. Hence, another metric which was used to evaluate the frame designs are the load-case dependent compliances. A single metric i.e. weighted compliance metric, which describes the sum of the individual compliance values for the load cases can be measured during a particular design iteration. It should be noted that the compliance of a structure is an inversed indication of the structure's stiffness, i.e. it can be concluded that a structure is stiff against a particular load-case if it exhibits a low compliance during that specific load-case.

The second last metric that will be used to evaluate frame performance is the body acceleration of the UAV frame under the given load-cases. These acceleration vectors change as the inertia of the frame is changed from iteration to iteration. By assessing the changes in magnitude and makeup, it is possible to draw conclusions regarding the changes in UAV manoeuvrability through the design process.

For qualitative purposes, the natural frequencies of the frame will be tracked through the various design iterations. This is important to ensure that the possibility of resonance between the frame and motors are considered and mitigated.

4.2 Design Evaluation and Discussion

Table 1 provides the data that will be used to evaluate the frame design in this section. The rest of this subsection will be dedicated to the mining of this data in order to churn it into evaluation information regarding the UAV frame design iterations.

Table 1: Design evaluation data.

Design Iteration	Mass (kg)	Weighted Compliance (m/N)	First 3 Natural Frequencies (Hz)
0 (Benchmark)	1.307	4.852974E-03	84.825, 103.963, 122.493
1	4.3473	6.9578442E-06	75.415, 118.285, 146.338
2	3.9628	1.0416215e-05	61.603, 105.028, 171.441
3	0.73926	1.310252E-03	27.916, 50.792, 59.631
4	0.647	5.902445E-03	28.537, 41.317, 47.003

4.2.1 Mass and Stiffness

Maximizing the frame stiffness was a requirement in the design process, but at the same time, it was necessary to keep the frame mass to a minimum. The former requirement calls for more material utilization while the latter calls for less material utilization in the design volume. The strategy for resolving these conflicting design actions was to maximize the frame stiffness while simultaneously hedging the design with an exact constraint on the mass of the frame. It was thus observed (and expected) that although compliance should have been minimized (equivalent to maximizing stiffness), it was inevitably increased from the benchmark through to the final iteration as a sacrifice for the achievement of the specification relating to the UAV mass. The compliance did, however, increase to a lesser degree than what the frame mass was minimized. This represents a design advantage which outweighs the associated disadvantage and is depicted in Figure 7. The figure depicts the two objective metrics used in this subsection to evaluate the frame performance (i.e. mass and weighted compliance) through the various design iterations. Notice that both metrics have been normalized against the benchmark concept.

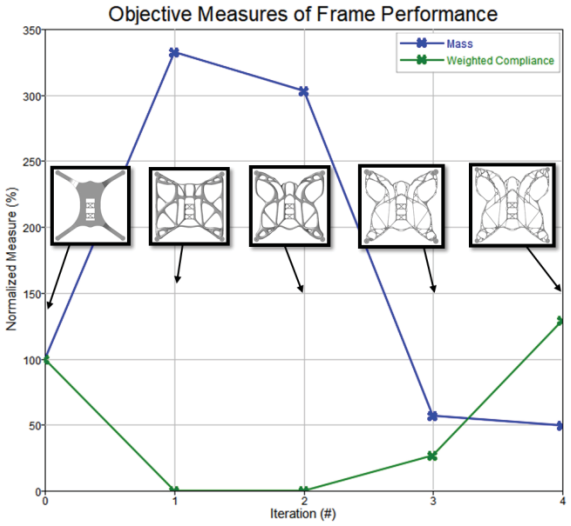

Figure 7: The normalized mass and stiffness trends through the design process.

Consider the following trends that can be observed in Figure .

- Notable changes in mass and stiffness from the benchmark to the first iteration can be seen. The most significant contributing factor is the change in material that has been affected (recall that the benchmark concept is made from Nylon whereas the final product is to be manufactured using Ti6Al4V).
- Iteration 1-2 marks almost no change in magnitude of stiffness, but almost 30% reduction in mass, signalling a significant design advantage gain. However, a significant transfer of stiffness from one load-case to another had taken place during this design iteration, see Section 4.2.2.
- Iteration 2-3 boasts an equally impressive design advantage: 246.6% mass reduction while only increasing compliance by 26.8%.
- Iteration 3-4 does not represent a design advantage since mass decreases by only 7% while compliance increases by 102%. The modifications made between these iterations, however, had been made based on manufacturing considerations.
- Benchmark vs. final design: Mass reduction of 50.5% with a simultaneous compliance increase of 29%. This represents an overall design advantage.

As was shown in Table 1, the frame weight specification has been met. The specification relating to stiffness has also been considered achieved since the frame stiffness has been maximized within the boundaries of the objective mass constraints.

4.2.2 Compliance per load-case

The global view of compliance in terms of its weighted sum which was considered in the previous subsection is further dissected in this subsection. Specifically, the implication of load-case dependent compliance changes are explored and the consequences explained. Consider Figure as an illustration of the observations that follow.

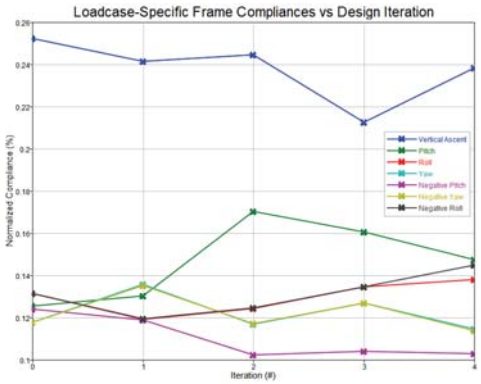

Figure 8: The normalized [per load-case] compliance through each design iteration.

Consider the following trends that can be observed in Figure .

- The load cases of positive and negative variants of distinct UAV motions (eg., pitch, roll, and yaw) create equal magnitudes of compliance in the structure except for pitch. The large difference in pitch/negative pitch compliance is attributed to the geometric asymmetry of the final design in the transverse plane which bisects the front and back halves of the UAV.
- The first load case (vertical ascent) accounts for most of the compliance in all of the iterations, thus influencing the designed topology most heavily of all the load-cases since all of the distinct loads (thrusts and torques) which combine to make up any one load-case are applied during ascent.
- The load-case which bears the lowest influence on the design is the negative pitching of the UAV (in all but the benchmark design).
- The negative pitching, yawing (both positive and negative) and vertical ascent load cases increased in stiffness while all other load cases became slightly more compliant. The effects of the former on the total weighted compliance (and thus the designed topology) of the frame, therefore, decreased while the effects of the latter were increased.
- Iteration 2-3 marked a big difference in compliance with the vertical load case: A large mass reduction was performed during this iteration.
- Iteration 1-2 marked a big increase in pitching compliance with a simultaneous decrease in negative pitching compliance: Aesthetic changes were made during this iteration.

The observations above are further augmented by considering the compliance profile of the benchmark and final design with reference to all seven load-cases. It can be seen in Figure 8 that the compliance profile with regards to the seven load-cases is similar in both the benchmark and the final design.

The most notable difference is that the final design exhibits more stiffness during negative pitching motions while simultaneously providing less stiffness during positive pitching motions. These large changes were realized between iterations 1 and 2, which are also shown in Figure 9.

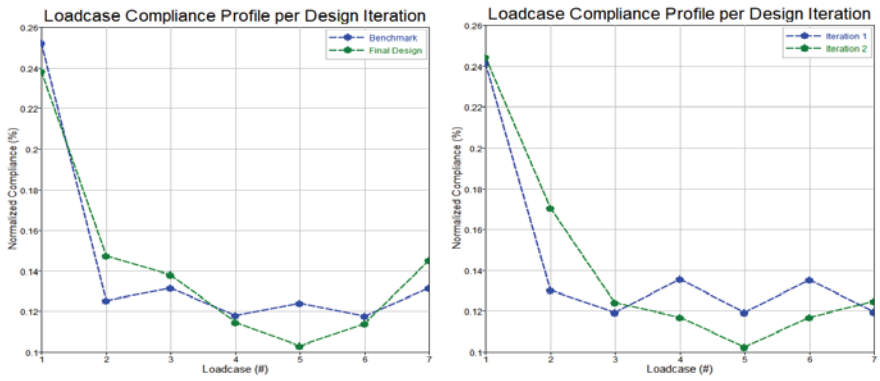

Figure 9: The load-case dependent compliance profiles of selected design iterations.

In conclusion, vertical ascent is the dominant design driver. Furthermore, the disparity in frame compliance during pitching/negative pitching is attributed to the frame's geometric asymmetry in the relevant plane. Large mass reductions caused large increases in vertical ascent compliance. Lastly, aesthetic changes caused large compliance changes in the pitching motion. Using the evaluation strategies laid out in Section 4.1, the authors consider the frame compliant regarding load-case dependent compliance. This is because, in the first place, the final requirement in Section **Error! Reference source not found.** called for the consideration of aesthetics during the design process. It was u

ncovered that the functional changes in UAV performance due to aesthetic changes in the UAV design were not adversely detrimental. Secondly, the load-case dependent compliances were tracked through the various iterations and although the changes were noted, they could not be classified as either improvements or deteriorations of the benchmark frame performance.

4.2.3 Linear and Rotational Acceleration

During the inertia relief analysis which supported this UAV design (see Section 2.1) it has been possible to extract the accelerations which are required to balance external forces from the analysis results. It is possible to draw conclusions about the changes in UAV manoeuvrability/dynamics by comparing these externally applied accelerations for the final and benchmarked models. The observations which follow are also coupled with the ones in Section 4.2.2, but it is much more intuitive to understand manoeuvrability changes from the perspective of balancing accelerations as opposed to weighted compliances. Consider Figure 10.

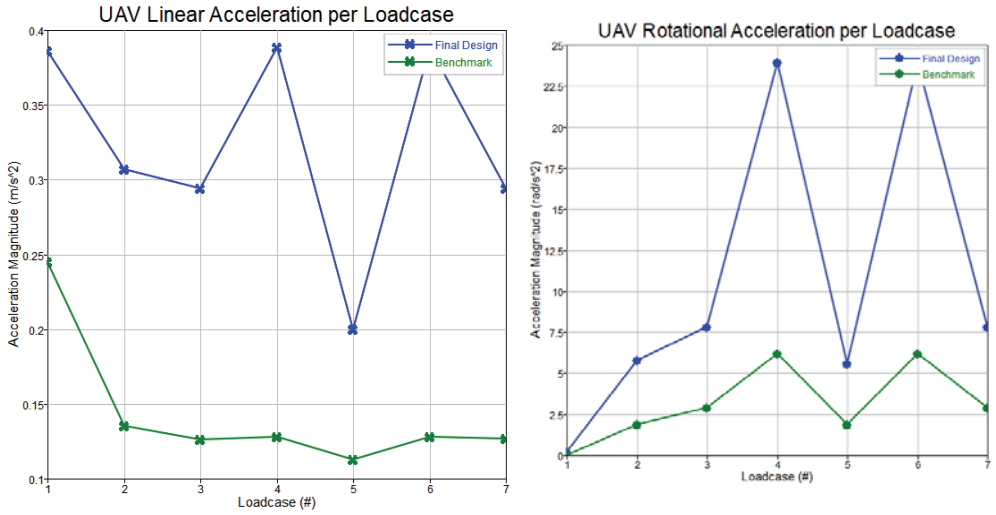

Figure 1: UAV accelerations per load-case for selected design iterations.

Consider the following observations that can be seen in **Error! Reference source not found.**

- The final design exhibits larger magnitudes in its linear and rotational accelerations. This can be attributed to the increased thrust-to-weight ratio relative to the benchmark.
- The vertical load-case causes the largest linear acceleration while simultaneously causing the smallest rotational acceleration in the benchmark.
- The yawing (positive and negative) load-cases cause linear accelerations similar in magnitude to the vertical load-case in the final design. The load-cases simultaneously cause large rotational accelerations, but this second part of this observation applies to the yawing load-cases in the benchmark case as well. The explanation for this is that in the final design, the COG has been shifted further from the intersection of the diagonals that connect the motors. Thus, thrust forces translate more efficiently into vertical ascent when applied across a single diagonal. However, during vertical ascent, since the motor positions are still not square, the combined thrust of all four motors translates into vertical ascent as well as a component of rotational acceleration which effectively dilutes the vertical ascent magnitude.
- The negative pitching load-case causes the lowest linear acceleration in both the benchmark and final design, although, in the case of the final design, the relative margin is higher between the magnitude of linear acceleration in the negative pitching load-case and all other load-cases.

In conclusion, the main inferences from these observations are that the UAV has become, on average, more manoeuvrable due to the increased thrust-to-weight ratio. Furthermore, the frame has become, relative to its other motions, more manoeuvrable in its yawing motions and less manoeuvrable in the negative pitching motion. The second of these conclusions will be influenced by the battery placement during assembly of the UAV. Thus, the two evaluation strategies laid out in Section 4.1 have been completed regarding frame acceleration since this subsection has successfully compared the various iterations and associated the comparisons with the thrust-to-weight ratio requirement given in Section 1.1.

4.2.4 Natural Frequencies

The change in natural frequencies for the first three natural modes of the structure is shown in Figure 11. Notice that the natural frequencies have been normalized by the baseline concept. Whereas the second and third modes increased slightly in the interim, they ultimately decreased. Comparing the benchmark and final design, it can be seen that all natural frequencies have been reduced in the range of 60-70%. This observation is of no consequence, however, since the excitation produced by the motors is to occur at frequencies far in excess of these natural modes and it is concluded that this metric has been successfully evaluated in terms of the strategy provided in Section 4.1.

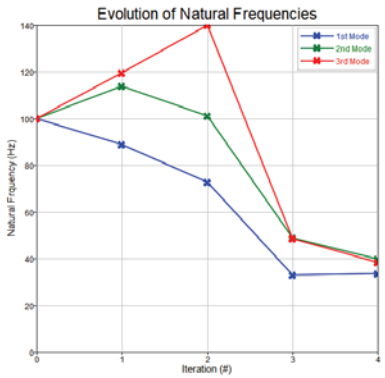

Figure 2: Evolution of the first three UAV frame natural frequencies.

5. CONCLUSION

A methodology for the mechanical design of a topologically optimized UAV frame was provided. The unique feature of the methodology which was developed is that it utilizes a two-step optimization process in which the first optimization serves to reduce the size of the computational problem while the second optimization becomes responsible for the generation of the final form of the UAV frame. The methodology was also injected with modifications to accommodate both aesthetic and manufacturability considerations. Since the design process was largely driven by simulation or virtual prototyping, the paper has provided details regarding the simulation technology and the inputs that have been submitted through the technology. These inputs included physical parameters such as material specifications and load definitions. The inputs also included considerations which affect the computation of the solution.

It was argued that in many of the simulations, trade-offs needed to be considered between accuracy and computation time. Lastly, the final frame design was evaluated utilizing a two-phase evaluation strategy. In the first phase, some evaluation metrics which can be determined, for each iteration of the UAV frame, during the design process. The metrics were then used to track changes through the design process and the final design was ultimately compared with the benchmark to conclude whether the design process had produced a result which was better than the benchmark. This was indeed the case. In the second phase, the metrics which could be associated with any of the UAV frame requirements set out in Section **Error! Reference source not found.** were used to settle those r equirements.

It was concluded that the UAV frame requirements were met, including frame weight, thrust to weight ratio and flight time all while maintaining frame stiffness. The optimized design solution, for the most part, minimizes features that will prevent the design from being printable with the powder bed fusion process on the Aeroswift machine. Topology optimization allowed for the development of a non-conventional frame while AM ensures manufacturability of this shape.

REFERENCES

[1] J. A. Benito, G. Glez-de-Rivera, J. Garrido and R. Ponticelli, "Design considerations of a small UAV platform carrying medium payloads," Design of Circuits and Integrated Systems, Madrid, 2014, pp. 1-6.

[2] A.V.Javir, K. Pawar, S. Dhudum, N. Patale,S. Patil, " Design, Analysis and Fabrication of Quadcopter," Journal of The International Association of Advanced Technology and Science, 2015.

[3] M. Mueller, "eCalc - the most reliable Multicopter Calculator on the Web", Ecalc.ch. [Online]. Available: https://www.ecalc.ch/xcoptercalc.php. [Accessed: 08- Jun- 2018].

[4] M. A. Khodja, M. Tadjine, M. S. Boucherit and M. Benzaoui, "Experimental dynamics identification and control of a quadcopter," 2017 6th International Conference on Systems and Control (ICSC), Batna, 2017, pp. 498-502.

[5] J. Apaza, D. Scipión, D. Lume and C. Saito, "Development of two UAVs for volcano studies in southern Peru," 2017 IEEE XXIV International Conference on Electronics, Electrical Engineering and Computing (INTERCON), Cusco, 2017, pp. 1-4.

[6] D. Munro, "A direct approach to structural topology optimization", Ph.D. dissertation, Dept. of Mechanical and Mechatronic Engineering, Stellebosch University, Stellenbosch, South Africa, 2017.

[7] Gibson, I., Rosen, D., Stucker, B. 2015. Additive Manufacturing Technologies, 2nd Edition, Springer-Verlag New York.

[8] Vatanabe, SL., Lippi, TN., de Lima, CR., Paulino, GH., Silva, CN. 2016. Topology optimization with manufacturing constraints: A unified projection-based approach, Advances in Engineering Software, 100(1), pp 97-112.

[9] Optistruct User Guide. 2017. [online]. Available: https://connect.altair.com/CP/kb-view.html?f=2&kb=167280 [Accessed: 19-June-2018].

[10] Gaynor, AT., Guest, JK. 2016. Topology optimization considering overhang constraints: Eliminating sacrificial support material in additive manufacturing through design, Structural and Multidisciplinary Optimiza**tion,** 54(5), pp 1157-1172.